MTLA 27 (2023) 101651

Contents lists available at ScienceDirect

Materialia

journal homepage: www.elsevier.com/locate/mtla

Full Length Article

Photoreactive Hydrogels Based on Type I Collagen Extracted from Different Sources as Scaffolds for Tissue Engineering Applications: A Comparative Study

Parisa Noohi [a,1], S. Sharareh Mahdavi [a,b,1], Mohammad J. Abdekhodaie [a,c,*], Mohammad H. Nekoofar [d,e,f], Alireza Baradaran-Rafii [g,h]

[a] Department of Chemical and Petroleum Engineering, Sharif University of Technology, Tehran, Iran
[b] Research Operations, The Hospital for Sick Children, Toronto, Canada
[c] Environmental and Applied Science Management, Yeates School of Graduate Studies, Toronto Metropolitan University, Toronto, Canada
[d] Department of Endodontics, School of Dentistry, Tehran University of Medical Sciences, Tehran, Iran
[e] Department of Tissue Engineering, School of Advanced Technologies in Medicine, Tehran University of Medical Sciences, Tehran, Iran
[f] Department of Endodontics, Bahçeşehir University School of Dentistry, Istanbul, Turkey
[g] Department of Ophthalmology, Morsani College of Medicine, University of South Florida, Tampa, Florida, USA
[h] Ophthalmic Research Centre, Shahid Beheshti University of Medical Sciences, Tehran, Iran

ARTICLE INFO

Keywords:
Bovine Achilles tendon
fish skin
rat tail
collagen methacrylate
PEG-diacrylate
hydrogels

ABSTRACT

Collagen-based hydrogels are promising constructs used frequently as scaffolds in various tissue engineering applications. The source of collagen extraction can influence the physiochemical properties, mechanical strength, as well as cellular behaviour of the tissue-engineered hydrogels. In the present study, type I collagen was isolated from three different animal sources, namely bovine Achilles tendon, bighead carp fish skin, and rat tail tendons. After characterizing the extracted collagens, their structures were modified via covalent functionalization of the free amines with methacrylate groups. Methacrylated collagens were combined with PEG-diacrylate to act as three-dimensional photocrosslinked scaffolds for culturing human corneal stromal cells. Physicochemical properties, mechanical strength, morphological features, and cellular behaviour were different depending on the collagen sources. Human corneal stromal cells more easily penetrated within hydrogels containing rat tail type I collagen, which also had greater pore sizes and porosity. However, the expressions of type I collagen and lumican were observed to be a greater extent in fish skin collagen-based hydrogels. Such observations highlight the significant effect of collagen extraction source on cellular behaviour and the importance of having a proper selection in accordance with the application of the tissue-engineered scaffold.

1. Introduction

Tissue engineering is an emerging interdisciplinary field that aims to regenerate damaged tissues by utilizing a combination of cells, signaling molecules, and polymeric scaffolds [1–4]. In this approach, developing a porous three-dimensional (3D) scaffold is crucial to mimic native extracellular matrices (ECMs) and to provide an appropriate microenvironment for optimal cell attachment, proliferation, and differentiation and regeneration of new healthy tissues [5,6]. Hydrogels hold remarkable potential as scaffolds in tissue engineering applications due to their porous structure, high water content, and tunable composition and physicochemical properties [7,8].

Type I collagen, which is the major structural building block of connective tissues, is a potential biomaterial to be used as the main component of scaffolds. Collagen supports cell attachment and initiates subsequent cellular responses [9]. Depending on the extraction source, the inherent chemical or physical properties of the collagen vary [10–12]. So far, type I collagen extracted from different animal sources has been used as the hydrogel basis. Smith et al. [13] used a direct-write bio-assembly system to fabricate viable structures in a layer-by-layer fashion using rat tail type I collagen. Although they obtained spatially well-organized structures as well as good cell viability, shortening the

* Corresponding author at: Department of Chemical and Petroleum Engineering, Sharif University of Technology, Tehran, Iran
E-mail address: abdmj@sharif.edu (M.J. Abdekhodaie).
[1] These authors have contributed equally.

https://doi.org/10.1016/j.mtla.2022.101651
Received 7 October 2022; Received in revised form 7 December 2022; Accepted 9 December 2022
Available online 11 December 2022

time of collagen fibrillogenesis resulted in the loss of mechanical integrity. In another study, rehydrated bovine collagen was applied as the bioink to create a structure with a spatial resolution of 500 μm using a developed nozzle-based 3D bioprinter [14]. Three-dimensional bioprinting is a promising approach to fabricate engineered hydrogels and offers several advantages, such as controlled cell distributions, high-resolution cell deposition, and scalability [15]. However, the slow gelation rate and poor mechanical strength of self-assembled collagen hydrogel restrict its applications in tissue engineering strategies [16]. To address these challenges, the use of chemically modified collagen has been of great interest in hydrogel synthesis.

So far, various crosslinking methods have been used to fabricate collagen-based constructs with improved mechanical integrity. For example, a porcine collagen-based bioink that was crosslinked by tannic acid (a polyphenol) was developed to fabricate 3D-printed cell-laden structures [17]. Also, genipin was tested as a crosslinker in the fabrication of a bovine collagen-based hydrogel for 3D cell encapsulation [18]. Among the reactive derivatives of collagen, photoreactive collagen has received much attention because of easy/fast gelation in the presence of a photoinitiator, tuneable mechanical properties, and controllable biodegradability. In addition, using photoreactive biomaterials provides a spatiotemporal control of crosslink formation by adjusting light exposure. To obtain photoreactive collagen, collagen methacrylate (ColMA) was synthesized through the reaction of its lysine residues with the methacrylic group in either methacrylic acid [19] or methacrylate anhydride [20]. Gaudet and Shreiber reported the superiority of hydrogels based on ColMA over those based on native collagen in terms of mechanical strength and biodegradability, while preserving cytocompatibility and self-assembling ability [19]. Using ColMA combined with thiolated hyaluronic acid as a bioink also indicated appropriate printability and biocompatibility as well as great mechanical strength [21,22].

In the present study, type I collagen was extracted from three different animal sources, including bovine Achilles tendon, bighead carp fish skin, and rat tail tendons, and their properties were compared. Next, the extracted collagens were modified via covalent functionalization of their free amines with methacrylate groups and used as photoreactive biomaterials to fabricate *in situ* forming hydrogels. To improve the mechanical strength, ColMA was combined with PEG-diacrylate (PEGDA). The physicochemical properties of engineered ColMA/PEGDA hydrogels as well as their mechanical properties and *in vitro* biocompatibility have been evaluated. Moreover, the effect of collagen extraction sources and light exposure time on these properties has been assessed. Also, cell migration through fabricated hydrogels containing ColMA derived from different sources and the protein expressions of the corneal stromal cells seeded on them have been investigated and compared.

2. Materials and Methods

2.1. Materials

Methacrylic anhydride, PEGDA, eosin Y (EY), triethanolamine (TEA), 1-vinyl-2-pyrrolidinone (NVP), 2,4,6-trinitrobenzenesulfonic acid (TNBS), pepsin from porcine gastric mucosa, acridine orange, propidium iodide, phosphate saline buffer (PBS), paraformaldehyde, and 4′,6- diamidino-2-phenylindole (DAPI) were purchased from Sigma-Aldrich, Germany. Dulbecco's modified eagle medium (DMEM), fetal bovine serum (FBS), penicillin-streptomycin (Penstrep), trypsin-EDTA (0.25%), collagenase type I, and 3-(4,5-dimethylthiazol-2-yl) 2,5diphenyltetrazolium bromide (MTT) were purchased from Gibco® Life Technologies, USA. All the other chemicals were purchased from Merck Millipore, Germany.

2.2. Collagen Extraction from Different Animal Sources

2.2.1. Bovine Achilles Tendon

Type I collagen was extracted from the bovine Achilles tendon based on the method developed by Delgado et al. [23]. Briefly, the isolated tendon was cryo-minced and washed with 1X phosphate buffered saline (PBS) solution. The minced tendon was dissolved in 0.5 M acetic acid containing 80 U porcine pepsin per mg of the minced tendon for enzymatic digestion. After 72 hours of dissolving under stirring, the resulting solution was filtered and centrifuged (6000 rpm for 30 minutes) to collect collagen solution. The soluble collagen was precipitated by adding 0.9 M NaCl. The precipitate was collected by centrifuging for 30 minutes at 6000 rpm, dissolved again in 0.5 M acetic acid, and dialyzed against 1 mM acetic acid. All processes were carried out at 4°C. The final product was obtained by freeze-drying for 48 hours.

2.2.2. Bighead Carp Fish Skin

The skin of the Persian Gulf bighead carp was selected as the marine source for the extraction of type I collagen. Briefly, the skin was washed with distilled water (dH_2O) and cut into small pieces. The pieces were treated with 0.1 M NaOH and 10% (v/v) ethanol, as described by Li et al. [24], to remove non-collagenous proteins and the fat, respectively. The treated skin pieces were dissolved in 0.5 M acetic acid under stirring for 72 hours. The resulting viscous solution was centrifuged at 6,000 rpm for 30 minutes to remove insoluble particles, and the supernatant was collected. Collagen precipitation occurred by adding 0.9 M NaCl, followed by centrifugation to collect precipitate. The precipitate was dissolved in 0.5 M acetic acid and dialyzed against 0.1 M acetic acid for 2 days and dH_2O for another 2 days. All processes were carried out at 4°C. Final fish collagen was obtained by freeze-drying the collagen solution for 48 hours.

2.2.3. Rat Tail Tendons

Type I collagen was extracted from rat tail tendons based on an established protocol [25]. Collagen fibres were removed from rat tail tendons and collected in 1X PBS. The fibres were immersed in acetone for 5 minutes, and 70% (v/v) isopropanol for another 5 minutes and dissolved in 0.02 M acetic acid on a magnetic stirrer for 72 hours. The resulting viscous solution was blended along with ice and centrifuged at 6,000 rpm to remove insoluble particles. The supernatant was collected and dialyzed against 0.02 M acetic acid for 5 days. All processes were carried out at 4°C. Finally, the acid-soluble type I collagen was obtained by freeze-drying the dialyzed solution for 48 hours.

2.3. Characterization of Extracted Collagens

2.3.1. Sodium Dodecyl Sulphate-Polyacrylamide Gel Electrophoresis (SDS-PAGE)

SDS-PAGE method was used based on an established protocol [26] to qualitatively analyse the purity of the extracted collagens. Briefly, 4 μl of collagen solutions with a concentration of 1 mg/ml in 0.5 M acetic acid were neutralized using 1 M NaOH. The resultant solutions were mixed with 42 μl of dH_2O and 12 μl of 5X sample buffer (containing SDS, Tris-HCl, dH_2O, glycerol, and bromophenol blue). Prepared samples were heated at 90°C for 5 minutes to denature. 5% (w/v) acrylamide gel as the running gel and 3% (w/v) stacking gel on top of it were prepared. Then, the gel plates were placed on the electrode bar, and the electrophoresis apparatus was assembled. Sample solutions were loaded into each well, and power was supplied (70 V, 60 minutes). Protein bands were obtained after staining with 0.1% (w/v) Coomassie blue and 12.5% (v/v) trichloroacetic acid and water treatment. Commercially available type I collagen isolated from bovine skin (Sigma-Aldrich, Germany) was used as the reference.

2.3.2. Formation of Physiological Hydrogel

The extracted collagens were physically polymerized to form self-

assembled hydrogels, as described previously [27]. Briefly, 0.41 ml of dH_2O containing 0.025 M NaOH was added to 0.1 ml 10X PBS at a pH of 7.4 on ice. Then, 0.49 ml of the collagen solution with a concentration of 8.16 mg/ml in 0.01 M acetic acid was added to the solution and mixed completely. Finally, the physiological hydrogel was formed by incubating the mixture at 37°C for 30 minutes.

2.3.3. Fourier Transform Infrared (FTIR) Spectroscopy

FTIR was carried out on dry samples using a Bruker Tensor 27 spectrophotometer (Germany). The spectra were obtained over the range of 400-4000 cm^{-1} with 20 scans.

2.3.4. Circular Dichroism (CD) Spectroscopy

The preservation of the triple helical architecture of samples was determined using the Aviv (model 215) CD spectrometer (USA). Samples with a concentration of 0.2 mg/ml were dissolved in 0.5 M acetic acid, and the CD measurements were carried out in 1.0 cm pathlength quartz cells at room temperature.

2.3.5. Ultraviolet/Visible (UV/VIS) Spectroscopy

UV/VIS absorption spectrum was acquired in a range of 190-490 nm using a UV/VIS spectrophotometer (Rayleigh UV2601, China). The sample solutions were extracted collagens in 0.5 M acetic acid with a concentration of 1 mg/ml.

2.3.6. (2,4,6)-Trinitrobenzenesulfonic Acid (TNBS) Colorimetric Assay

Free amines available on the backbone of the extracted collagens were determined using TNBS colorimetric assay, as described earlier with a slight modification [26]. Briefly, 3 mg of dry samples were immersed in 500 µl of 0.1 M sodium bicarbonate, and 250 µl of 0.5% (w/v) TNBS was added to the mixture. Four hours after the reaction under mild orbital shaking (150 rpm, 37°C), 250 µl of 10% (w/v) sodium dodecyl sulfate (SDS) and 125 µl of 1 M HCl were added to the mixture to stop the reaction. Sample residues were completely dissolved through hydrolysis at 120°C for 30 minutes. Then, the absorbance of the sample solutions was read at 405 nm. Lysine was used as the standard solution to determine the molar content of free amine groups in the extracted collagens, and the calibration curve was obtained by measuring the absorbance of lysine solutions with specified concentrations (0-0.22 mg/ml with 0.02 interval).

2.4. Synthesis of Collagen Methacrylate (ColMA)

Extracted collagens from each source (0.25% (w/v)) were dissolved in 5 mM dimethyl sulfoxide (DMSO) at 4°C until complete dissolution. Methacrylic anhydride was added dropwise to the solution in proportion to the calculated moles of free amines presented in the backbone of each collagen. After 24 hours of reaction, the reaction mixture was dialyzed against dH_2O for 5 days. The dialysate was changed twice a day. Finally, ColMA was recovered by freeze-drying.

2.5. Photoactivation and Hydrogel Formation

ColMA/PEGDA hydrogel was formed via photocrosslinking using a protocol established by the CellInk company [28] with a slight modification. Briefly, ColMA and PEGDA were dissolved in 2 mM acetic acid at 4°C as follow:

$$V_{\text{Acetic acid+PEGDA}} = \left(C_{f,\text{ColMA}} \times V_{\text{Hydrogel}}\right) / C_{i,\text{ColMA}}$$

where $C_{f,\text{ColMA}}$, V_{Hydrogel}, and $C_{i,\text{ColMA}}$ are the final concentration of ColMA in the precursor solution (5 mg/ml), the final volume of the hydrogel (1 ml), and the initial concentration of ColMA in the solution (7 mg/ml), respectively. $V_{\text{Acetic acid+PEGDA}}$ is also the total volume of acetic acid and PEGDA. The final concentration of PEGDA in the precursor solution was considered 5% (w/v). Then, a mixture containing specific volumes of 10X PBS ($V_{10X\ PBS}$), NaOH (V_{NaOH}), dH_2O (V_{dH_2O}), and photoinitiator (V_{PI}) was added to the solution to neutralize pH as follow:

$$V_{10X\ PBS} = 0.1 \times V_{\text{Hydrogel}}$$

$$V_{NaOH} = 0.011 \times V_{\text{Acetic acid+PEGDA}}$$

$$V_{dH_2O} = V_{\text{Hydrogel}} - V_{\text{Acetic acid+PEGDA}} - V_{10X\ PBS} - V_{NaOH} - V_{PI}$$

The base concentration of the photoinitiator mixture was 0.1 mM EY (as the photoinitiator), 1.5% (w/v) TEA (as the co-initiator), and 0.5% (w/v) NVP (as the co-monomer). To avoid unexpected dilution, EY was dissolved in 10X PBS. Also, the TEA solution was neutralized with HCl to prevent collagen precipitation. After homogenising the mixture of ColMA/PEGDA with neutralizing solution, the obtained solution was poured into a cylindrical mould with a diameter of 8 mm and a height of 3 mm and exposed to visible light using an increasing range of times (30, 60, and 90 seconds) to form light-curing hydrogels. Homogenisation was carried out via rapid pipetting of the mixture up and down several times to prevent unwanted gelation of collagen. Light-induced polymerization was carried out using a LED.D curing light (Woodpecker, China) with a wavelength of 440-490 nm and an intensity of 1000 ~ 1200 mW/cm^2.

2.6. Hydrogel Characterization

2.6.1. Chemical Characterization

Proton nuclear magnetic resonance (^1H NMR) spectroscopy was used to investigate the functionalization of the extracted collagens. Lyophilized native collagens and methacrylated collagens (10 mg/ml) were dissolved in deuterated DMSO overnight, and the spectra were recorded using a Bruker DRX-500 AVANCE spectrometer (Bruker BioSpin AG, Switzerland). The degree of methacrylation (DOM) was calculated as described previously [29].

FTIR and CD spectroscopies were also used to characterize and to evaluate the preservation of triple helical architecture of the methacrylated collagens as described above.

2.6.2. Physical Characterization

2.6.2.1. Swelling Ratio. To assess the swelling ratio of photocrosslinked hydrogels, cylindrical hydrogels with ~8 mm diameter and ~3 mm thickness were prepared and weighed immediately after crosslinking and again after 24 hours of swelling in 1X PBS at 37°C [30]. The percentage of effective swelling was reported by calculating the difference between the measured weights.

2.6.2.2. Enzymatic Degradation. The enzymatic degradation test was carried out as described in the previous work [31]. Briefly, prepared hydrogels with specified weights were incubated in 1X PBS and 50 U/ml of collagenase type I isolated from Clostridium histolyticum at 37°C. At specific time intervals (24, 48, 72, 96, and 144 hours), mixtures were centrifuged at 6000 rpm for 5 minutes, and the remnants of the samples were weighed. The degradation rate was determined by calculating the mass difference between samples before and after degradation.

2.6.3. Mechanical Characterization

The compressive Young's modulus of hydrogels was determined using a universal mechanical testing machine (Hounsfield-H10KS, USA) with a 50 kN load cell. The hydrogels were prepared using cylindrical moulds with a diameter of 8 mm and a height of 6 mm and incubated in PBS at 37°C before the test. Compression tests were carried out at 1 mm/min, and Young's modulus was determined as the slope of the linear region of the stress-strain curve.

2.6.4. Morphological Characterization

After gold sputtering, the interior morphologies of freeze-dried hydrogels were observed by scanning electron microscopy (Philips

XL30 ESEM, Netherlands). Images were taken and analysed using ImageJ software (NIH, USA) to determine the pore size and the porosity of each photocrosslinked hydrogel.

2.7. In Vitro Cellular Studies

2.7.1. Cell Isolation

Two different types of cells were used, including human dental pulp stem cells (hDPSCs) and human corneal stromal cells (hCSCs). hDPSCs were supplied by Royan Biotechnology Research Institute (Iran), while hCSCs were isolated from corneal stromal tissue as described previously [32,33]. Human corneal stromal tissues were obtained from Labfi Nejad Hospital (Tehran, Iran), as approved by the Iran National Committee for Ethics in Biomedical Research (Study ID: IR.SBMU.ORC.REC.1398.010). Briefly, the tissues were cut into ~2 mm × 2 mm pieces using an ophthalmic scissor. The tissue fragments were incubated in 2 mg/ml collagenase type I solution to digest enzymatically for 2 hours at 37°C. The mixture was centrifuged at 1500 rpm for 5 minutes, and the supernatant was discarded. The collected tissue pieces were incubated in 0.25% trypsin-EDTA for 5 minutes at 37°C. The isolated cells were collected by centrifuging and cultured in a 25-cm^2 culture flask in DMEM/F12 supplemented with 10% FBS and 1% Pensterp. hCSCs and hDPSCs were used after passage 3 and passage 5, respectively.

2.7.2. MTT Assay

In vitro cell viability was measured through MTT colorimetric assay. The hydrogel precursor solution was prepared as described above. Then, 150 µl of the prepolymer solution was placed into a cylindrical mould (8 mm in diameter and 3 mm in height) and photocrosslinked upon exposure to visible light for specified times (30, 60, and 90 seconds). The prepared samples were transferred to a 48-well culture plate and 6 µl of hCSCs suspension (2.5×10^6 cells/ml) was seeded on each sample. After 45 minutes of incubation at 37°C and 5% CO_2, 400 µl of the cell culture medium was added to each well. The same density of hCSCs was seeded on the culture plate (without hydrogel) as the control group. The culture media were changed every other day. After 1, 3, 5, and 7 days of incubation, the culture medium was removed, and 250 µl DMEM containing 10% MTT dye (5 mg/ml in RPMI1640) was added to each well. Incubation was carried out for 4 hours at 37°C to ensure the formation of formazan crystals. Then, the MTT solution was aspirated, and DMSO was added to elute the insoluble formazan. After incubation overnight under shaking, hydrogels were removed, and the absorbance of the solutions was measured at 490 nm using a microplate enzyme-linked immunosorbent assay (ELISA) reader (ELx800, BioTek Instruments Inc., USA). The assay was repeated in five replications.

2.7.3. Cell Migration via Live/Dead Assay

The migration of seeded cells within the photocrosslinked hydrogels was investigated via live/dead assay. Both types of cells, i.e. hDPSCs and hCSCs, were used in this assessment. Cell seeded hydrogels were incubated at 37°C and 5% CO_2 for 24 hours. To assess the penetration depth of seeded cells within photocrosslinked hydrogels, samples were incubated for 15 minutes with acridine orange at room temperature. Next, samples were washed three times with PBS and incubated with propidium iodide for another 15 minutes. After several steps of washing, the stained samples were observed under an inverted fluorescence microscope (Olympus, Japan). To measure the penetration depth of cells, ImageJ software was used.

2.7.4. Immunohistochemistry

Expression of lumican (Lum) and type I collagen (Col I) were visualized using immunohistochemistry. After 30 days of *in vitro* culturing, cell-seeded hydrogels were fixed using 4% paraformaldehyde for 20 minutes and then washed with PBS three times. Next, the cell membrane was made permeable by adding 0.3% Triton X-100. After 30 minutes, samples were washed with PBS and incubated in 10% goat serum (G9023, Sigma-Aldrich, Germany) as a blocking buffer to block the secondary antibody. After 45 minutes, the blocking solution was removed, and the primary antibodies (rabbit anti-lumican (orb100104) and mouse anti-collagen type I (orb375159), Biorbyt, UK) at a 1:100 dilution were added. Samples were incubated for 24 hours at 4°C and washed 4 times with PBS afterward. Next, the secondary antibodies (goat anti-rabbit IgG antibody (PE) (orb735029) and goat anti-mouse IgG(H+L) antibody (FITC) (orb688924), Biorbyt, UK) at a 1:150 dilution were added, and samples were incubated at 37°C and 5% CO_2 for 90 minutes in the dark. After washing 3 times with PBS, samples were stained with DAPI for 20 minutes, and immunoreactivity was visualized using an Olympus fluorescent microscope.

2.8. Statistical Analysis

All experiments were performed with three replications unless indicated. The results were presented as the mean ± standard deviation (SD). Statistical significance of the obtained data was analysed using a one-way analysis of variance (ANOVA) followed by Turkey's post hoc analysis. Differences were taken to be significant for *p-value < 0.05, **p-value < 0.01, ***p-value < 0.001, and ****p-value < 0.0001.

3. Results

3.1. Characterization of Extracted Collagens

Acid solubilized collagen was extracted from various sources, including bovine Achilles tendon, bighead carp fish skin, and rat tail tendons. The subunit composition and type of extracted collagens were assessed with SDS-page analysis. The patterns for collagens extracted from each source along with that for commercially-available type I collagen from bovine skin as a reference are shown in Fig. 1A. For all samples, the typical band pattern of type I collagen, including a doublet at apparent molecular masses around 130 kDa for two different kinds of α-chains (α_1 and α_2) and bands at higher molecular mass, above 200 kDa, for β and γ chain components, were observed. The purity of the extracted collagens was also verified by UV/VIS absorption spectra via getting a maximum absorption peak at 233 nm for all samples, as shown in Fig. 1B. Moreover, typical bands for type I collagen including amide A, amide B, amide I, amide II, and amide III were represented by the FTIR spectra of the isolated collagens that are shown in Fig. 1C. For all collagen samples, the amide A band was positioned between 3319 to 3330 cm^{-1}. Amide B band appeared between 2930-2960 cm^{-1}, which was similar to the wavenumbers reported for type I collagen extracted from other sources [24,34,35]. Amide I, amide II, and amide III bands were also found at wavenumbers around 1653, 1545, and 1240 cm^{-1}, respectively. Similar wavenumbers were reported for such bands obtained for type I collagen extracted from the eel fish skin [36], bovine pericardium [37], and human placenta [38]. Also, the preservation of the triple helical architecture of the extracted collagens was verified using CD spectroscopy (Fig. 1D) through observation of a positive band around 221 nm and a large negative peak around 198 nm for each sample.

In addition, the self-assembly of extracted collagens into a fibrillar gel, which is an intrinsic property of type I collagen, was observed at physiological pH and temperature. The behaviour of physiological hydrogels was different for various collagens. As shown in Fig. S1A (Supplementary Material), collagens extracted from rat and fish sources were formable and self-assembled in the shape of microtubes, while bovine collagen hydrogel contracted and took on an irregular shape. Morphological analysis via SEM imaging also revealed that the porosity and pore sizes were different between sources and, as expected, bovine hydrogel had the smallest pore size and the lowest porosity (Fig. S1B, Supplementary Material). It is worth mentioning that the lower denaturation temperature of fish collagen (~20-30°C [11,39,40]) than physiological temperature (37°C) led to the loss of stability of its

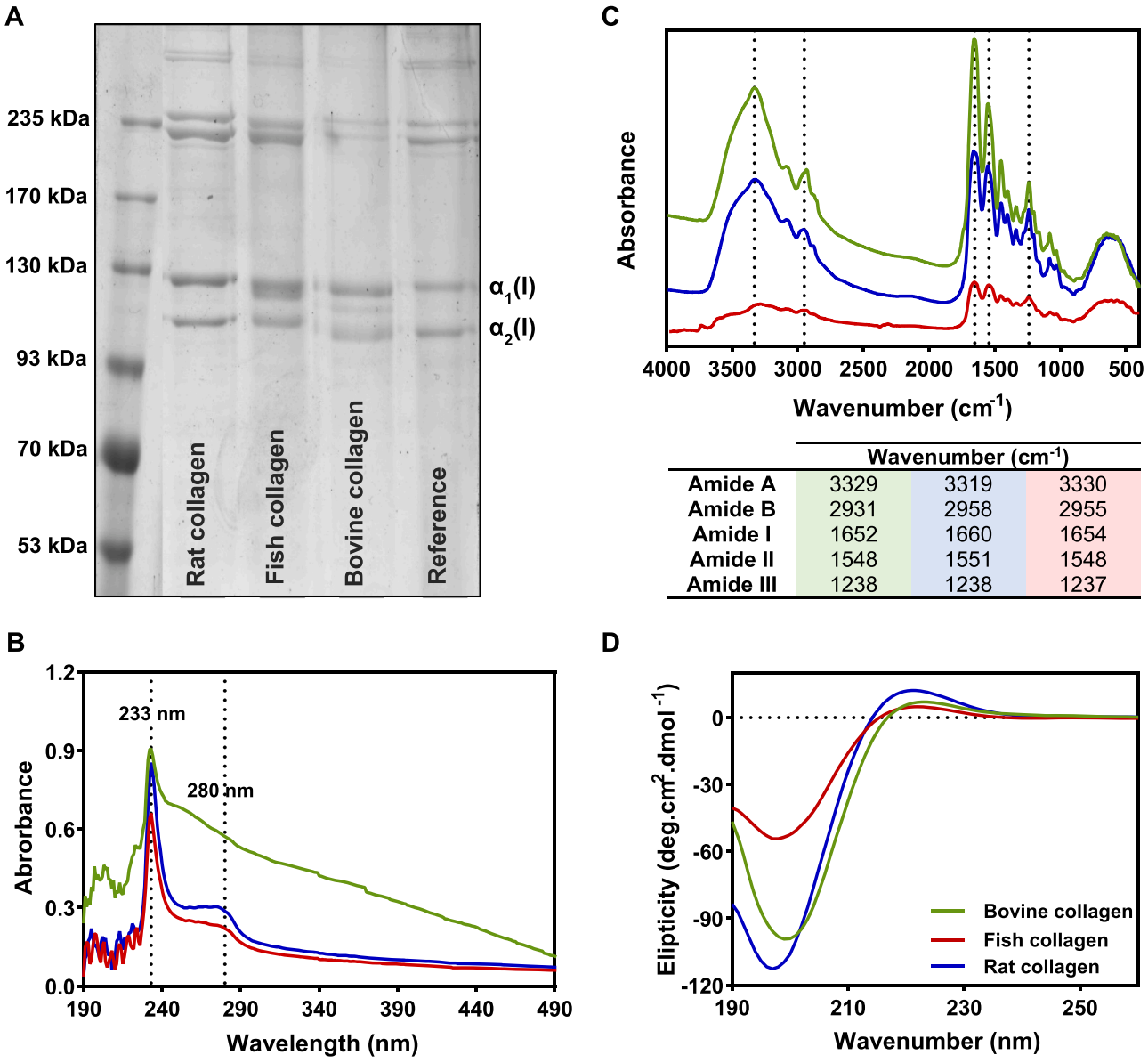

	Wavenumber (cm^{-1})		
Amide A	3329	3319	3330
Amide B	2931	2958	2955
Amide I	1652	1660	1654
Amide II	1548	1551	1548
Amide III	1238	1238	1237

Fig. 1. Characterization of type I collagen extracted from different sources. (A) SDS-PAGE of isolated collagens and commercially available type I collagen from bovine skin (Sigma-Aldrich) as the reference. (B) UV/VIS, (C) FTIR, and (D) CD spectra of isolated collagens.

self-assembled hydrogel within a short period of time (data not presented).

3.2. Optimization and Characterization of Photocrosslinked Hydrogels

Isolated collagens from different sources were functionalized with methacrylic anhydride to prepare photoreactive biomaterials. In this method, collagen was functionalized through covalent binding of methacrylic moieties with free amino groups of collagens, which were determined via TNBS colorimetric assay (Fig. S2, Supplementary Material). Type I collagen isolated from bovine, fish, and rat presented 2.836×10^{-4}, 2.744×10^{-4}, and 3.381×10^{-4} moles of lysine per gram, respectively, which were similar to the lysine content previously reported for collagen isolated from such sources [41–43]. The reaction of isolated collagens with methacrylic anhydride was conducted with a constant methacrylic-to-lysine ratio, and the DOM for three collagen samples was calculated by ^{1}H NMR. As shown in Fig. 2A, the characteristic peaks of methacrylic moieties (5.3 and 5.6 ppm [19,20]) were observed in the ^{1}H NMR spectrum of all samples. The DOM was calculated to be around 42, 51, and 60% for fish, bovine, and rat collagens, respectively.

In addition to methacrylation yield, the effect of functionalization on the triple helical structure of collagen samples was also addressed via CD spectroscopy. A positive peak at 221 nm and a negative peak at 198 nm, which are the characteristic peaks of collagen triple helices and polyproline chains, respectively [44], were observed for all modified samples as in the case of isolated collagens (Fig. 2B). In CD spectra, the ratio of positive peak intensity over negative peak intensity is defined as a useful parameter, called RPN, that indicates the preservation of triple-helical conformations [44]. This value, as reported in Fig. 2B, was comparable between methacrylated collagen and native collagen for all sources that illustrated the maintenance of triple-helices during the methacrylation process.

To form bicomponent *in situ* forming hydrogels, ColMA and PEGDA were dissolved in acetic acid and after addition of the neutralizing solution containing photoinitiators, photocrosslinked as shown in Fig. 3A. For determining the optimal light exposure time to fabricate hydrogels with suitable properties, different samples were synthesized under

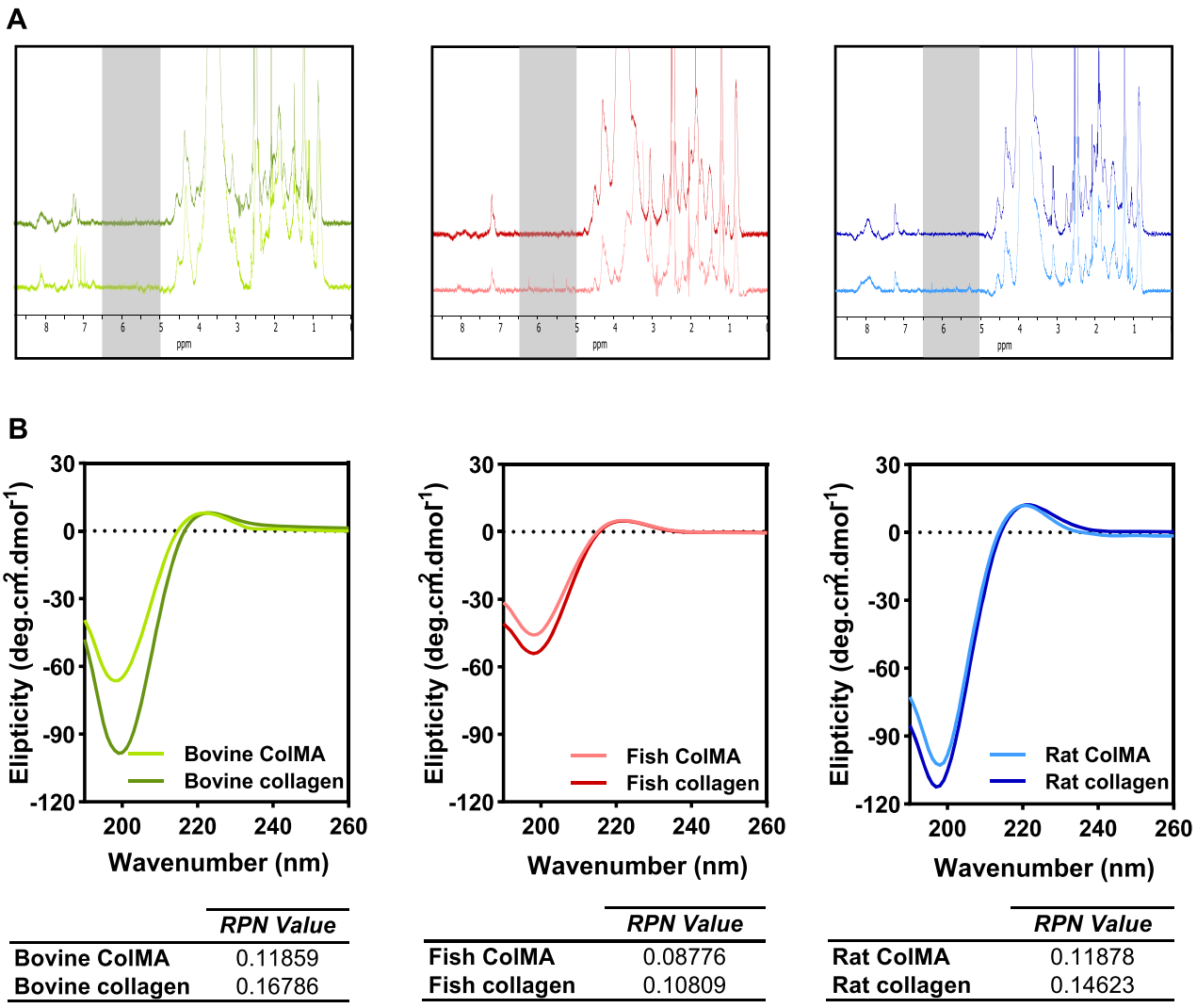

	RPN Value
Bovine ColMA	0.11859
Bovine collagen	0.16786

	RPN Value
Fish ColMA	0.08776
Fish collagen	0.10809

	RPN Value
Rat ColMA	0.11878
Rat collagen	0.14623

Fig. 2. Characterization of methacrylated type I collagen from each source. (A) ^{1}H NMR spectra of isolated collagen and ColMA form each animal source. The grey band represents the characteristic peaks of methacrylic moieties, if any. (B) CD spectra of isolated collagen and ColMA form each animal source.

various light exposure times (30, 60, and 90 seconds), and their mechanical strength, morphological properties, and cytocompatibility were compared. Obviously, the mechanical strength of all kinds of ColMA/PEGDA hydrogels was increased as the time of light exposure increased (Fig. 3B). Increasing light exposure time from 30 to 90 seconds led to the enhancement of Young's modulus from 20.3 ± 0.8, 17.1 ± 0.2, and 24.6 ± 0.9 kPa to 37.5 ± 2.6, 30.9 ± 1.2, and 46.6 ± 2.4 kPa for the hydrogels containing bovine, fish, and rat ColMA, respectively. However, MTT analysis after 7 days of *in vitro* culturing revealed that seeded hCSCs exhibited slightly lower viability on the hydrogels cross-linked upon longer exposure times (Fig. 3C). As an example, by the enhancement of light exposure time from 30 to 90 seconds, cell viability on the hydrogels containing bovine ColMA decreased from 163.8 ± 11.9% to 144.9 ± 6.5%. In addition, the morphological analysis indicated that the pore size and porosity of the hydrogels decreased with increasing light exposure time (Fig. 3D&E). The pore size of bicomponent hydrogels containing bovine ColMA was 128.5 ± 11.1 μm, 113.5 ± 11.3 μm, and 57.5 ± 6.2 μm for the light exposure time of 30, 60, and 90 seconds. Considering these observations, 60 seconds of light exposure was selected as the optimal light exposure time for further investigation.

As shown in Fig. 4A, Young's modulus of optimized hydrogels varied according to the extraction source of collagen. The greatest Young's modulus was belong to bicomponent hydrogels based on type I collagen isolated from rat tail tendons (32.8 ± 1.6 kPa), whereas those based on marine collagen exhibited the weakest mechanical strength (24.4 ± 0.8 kPa). Similar results were obtained from the *in vitro* enzymatic degradation test, where hydrogels were incubated in collagenase type I solution (10 U/ml) for 6 days (Fig. 4B). Using marine collagen in the structure accelerated degradation as compared with using collagens isolated from the other two sources. In particular, hydrogels based on marine collagen showed 93.3 ± 3.2% degradation at day 6 post incubation, while 88.5 ± 6.0% and 85.2 ± 6.7% of the hydrogels containing bovine and rat collagen, respectively, were degraded during the same time. Also, the water uptake capacity of optimal samples was determined after 24 hours of incubation in PBS. As shown in Fig. 4C, the effective swelling ratio was different between these samples, and the greatest ratio (16.2 ± 1.4%) was obtained for marine collagen-based hydrogels. This ratio was 6.7 ± 0.9% and 12.5 ± 1.5% for bovine collagen- and rat collagen-based hydrogels, respectively.

3.3. Cellular Studies

The cytocompatibility of optimized ColMA/PEGDA hydrogels containing ColMA from different sources was investigated and compared using MTT assay on days 1, 3, 5, and 7. In this regard, the 2D culture of hCSCs on a tissue culture plate was considered as the control group. As

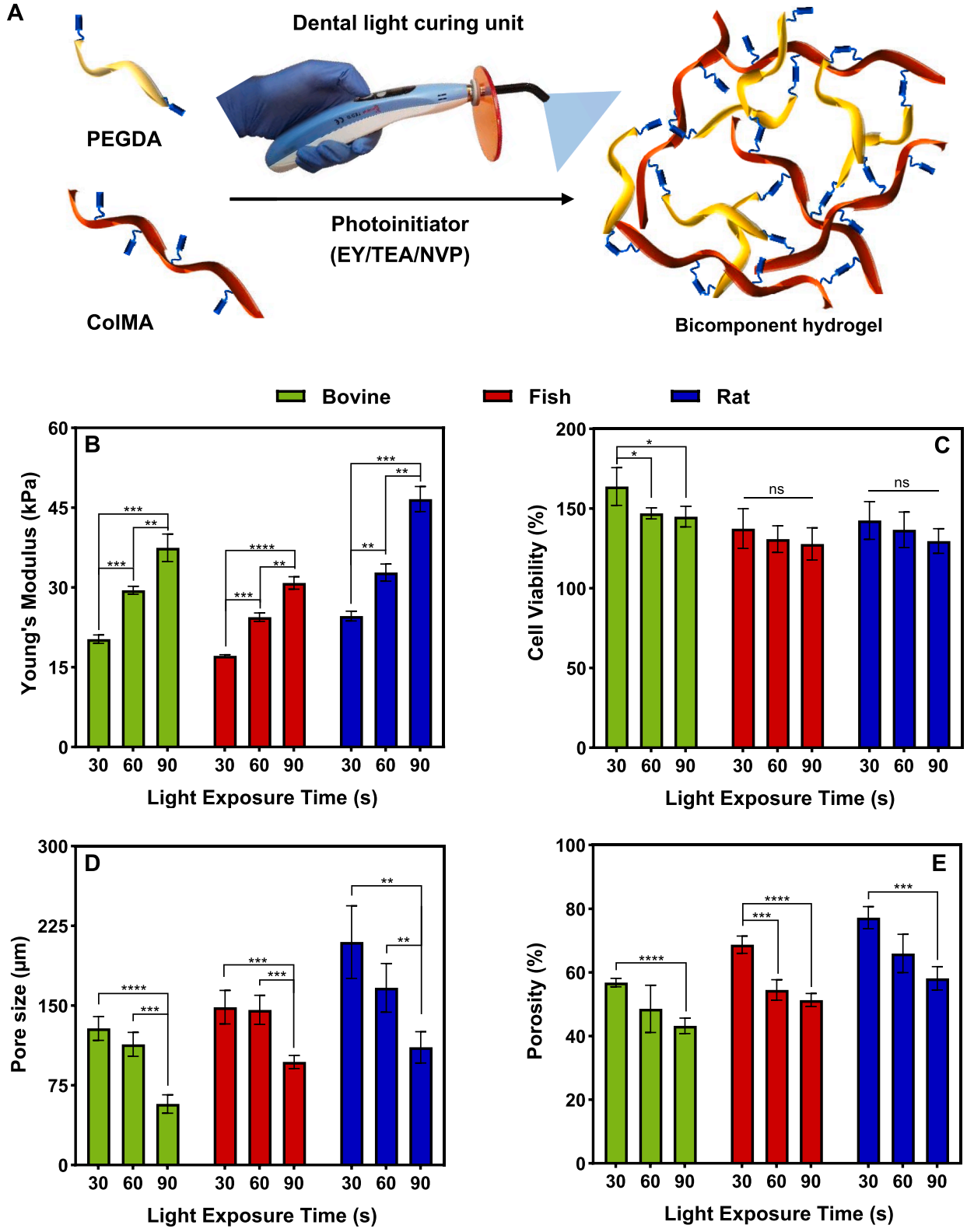

Fig. 3. Optimization of bicomponent hydrogels. (A) Synthesis and photocrosslinking process of bicomponent ColMA/PEGDA hydrogels. (B) Young's modulus, (C) cell viability, (D) pore size, and (E) porosity of the bicomponent hydrogels fabricated under different light exposure times. Data are presented as mean ± SD (*$p < 0.05$, **$p < 0.01$, ***$p < 0.001$, ****$p < 0.0001$, ns: not significant).

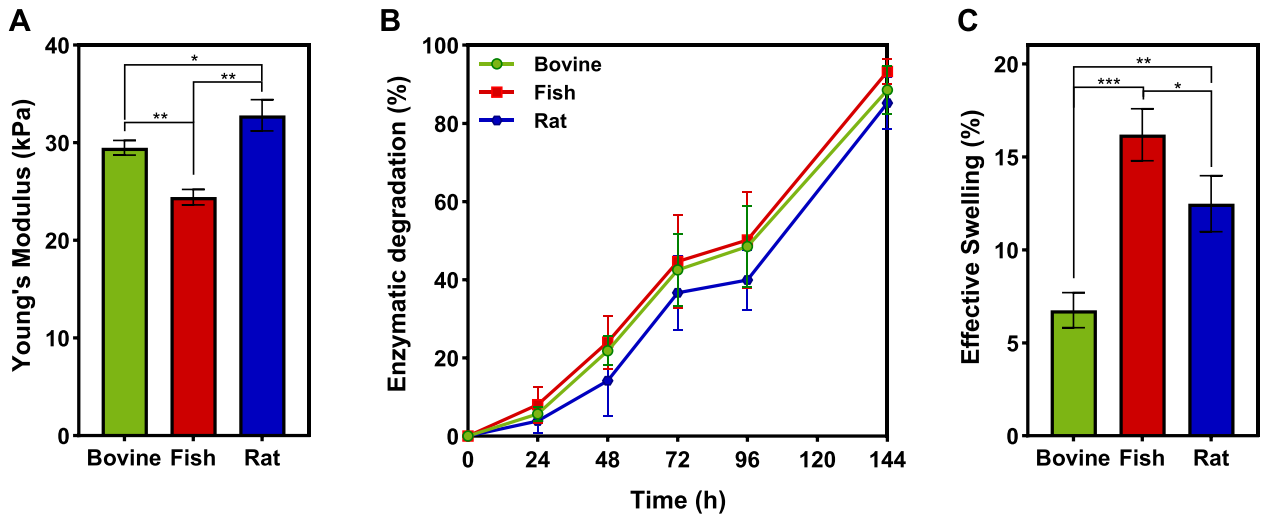

Fig. 4. Characterization of optimized hydrogels containing ColMA from different extraction sources. (A) Young's modulus, (B) enzymatic degradation, and (C) effective swelling ratio of the bicomponent hydrogels fabricated upon 60 seconds of light exposure. Data are presented as mean ± SD (*p < 0.05, **p < 0.01, ***p < 0.001).

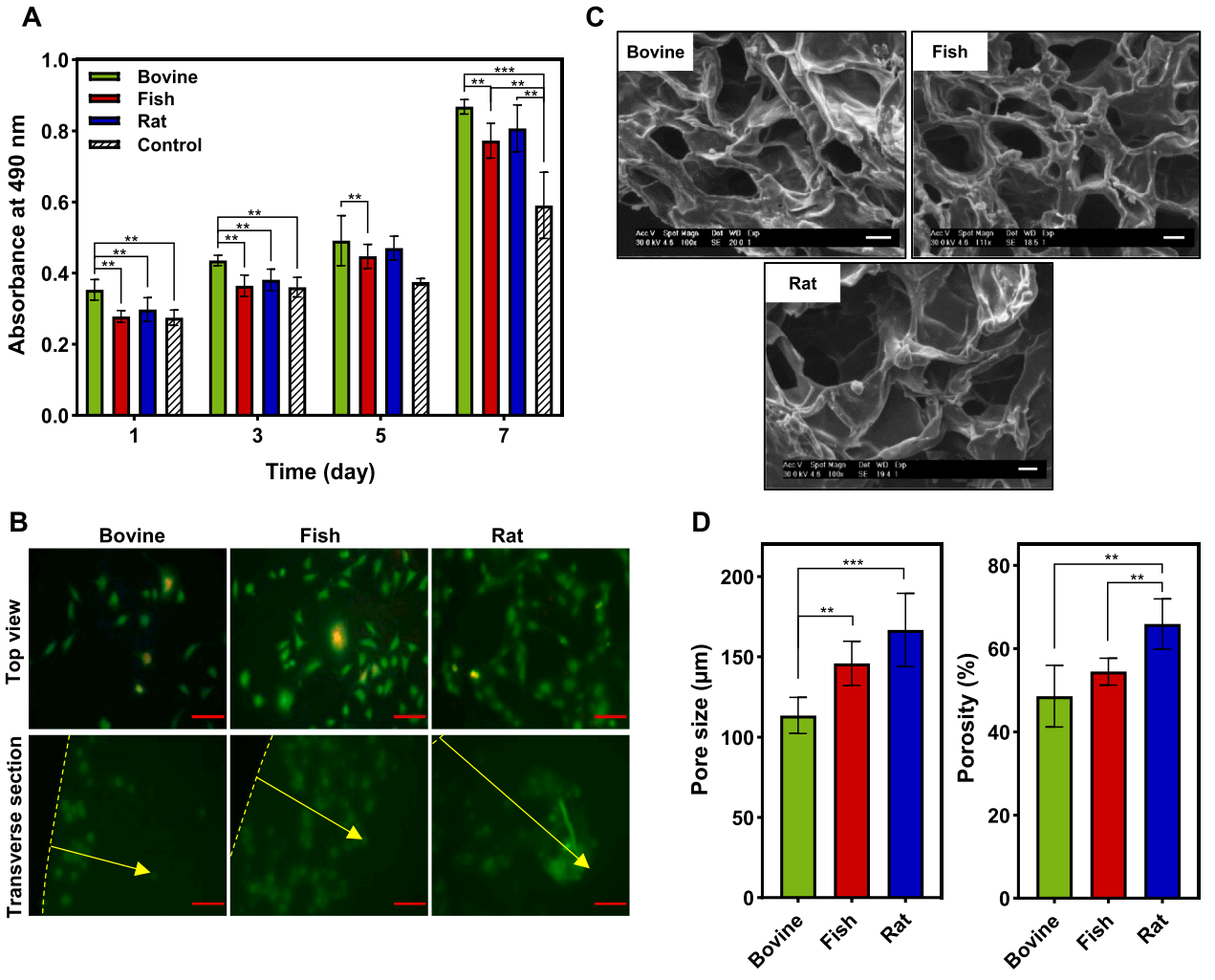

Fig. 5. *In vitro*cell culturing and morphological properties ofoptimized hydrogels. (A) Viability of hCSCs seeded on biocomponent hydrogels after 1, 3, 5, and 7 days obtained from MTT assay. (B) Representative live/dead images of hCSCs seeded on biocomponent hydrogels after 24 hours (scale bar: 100 μm). The dashed lines and yellow arrows show the gel surface and cell penetration depth within hydrogels, respectively. (C) Representative SEM images of the cross-section of bicomponent hydrogels (scale bar: 200 μm) and (D) their morphological properties. Data are presented as mean ± SD (**p < 0.01, ***p < 0.001).

illustrated in Fig. 5A, optical density values corresponding to formazan solutions highlighted an upward trend in the viability of cells seeded on all kinds of ColMA/PEGDA hydrogels over time. Additionally, relative percentages of cytocompatibility revealed that cells proliferated in all the samples. In particular, after 7 days of incubation, cell viability reached 147.0 ± 3.5%, 130.8 ± 8.3%, and 136.7 ± 11.5% for hydrogels based on bovine, fish, and rat ColMA, respectively. Comparison between various sources indicated that hCSCs had greater viability and proliferation when seeded on bicomponent hydrogel based on bovine ColMA.

Distribution of hCSCs on the optimized hydrogels and their migration within them was also compared via live/dead staining assay. In this respect, hCSCs were seeded on top of the optimized hydrogels based on various sources of ColMA, and cell distribution and penetration depth within different samples were compared after 24 hours. Fig. 5B shows the top view and the transverse section of cell-seeded samples. All of the bicomponent hydrogels supported the attachment, viability, and penetration of hCSCs. However, the extraction source of collagen affected cell migration through hydrogels. Hydrogels based on rat ColMA facilitated cell migration in comparison with hydrogels based on ColMA derived from the other two sources. Similar results were observed after seeding DPSCs on the top of optimized samples, where cell penetration depth within hydrogels based on rat ColMA was 2.8 and 1.4 times greater than that based on fish and bovine ColMA, respectively (Fig. S3, Supplementary Material).

The effect of collagen sources on the protein expression by hCSCs seeded on optimized samples was also investigated after 30 days of incubation. In this regard, the secretion of Lum and Col I was visualized via immunohistochemistry (Fig. 6). Interestingly, cells seeded on optimized hydrogels based on ColMA extracted from different sources had different patterns of protein production. The greatest expression of Col I was about 79%, which was observed for samples containing fish ColMA, while it was about 73% and 67% for samples containing bovine and rat ColMA, respectively. A similar trend was observed for the expression of LUM, which was about 77%, 70%, and 61% for samples based on fish, bovine, and rat, respectively.

4. Discussion

Versatile properties of type I collagen including biodegradability and excellent biocompatibility make it a promising scaffold basis to engineer various tissues such as cornea, cartilage, bone, skin, and dental tissues. However, the collagen extraction source might change its characteristics such as its aminoacidic composition and physical properties [10], which in turn may affect the properties of the obtained scaffolds. Bovine, rat, and marine collagens represent readily available sources for use in tissue engineering applications. Bovine is the most common source of collagen extraction for clinical use, while rat collagen is mostly used for tissue engineering research. The risk of disease transmission, allergenic responses, and religious and ethical constraints have limited the clinical use of rat collagen [45,46]. In the past decade, marine sources, especially fishes, have attracted much attention as an alternative safe source. Fish by-products, such as scales, bones, and skin, are rich in collagen. The present study was designed to compare characteristics of type I collagen extracted from bovine Achilles tendon, bighead carp fish skin,

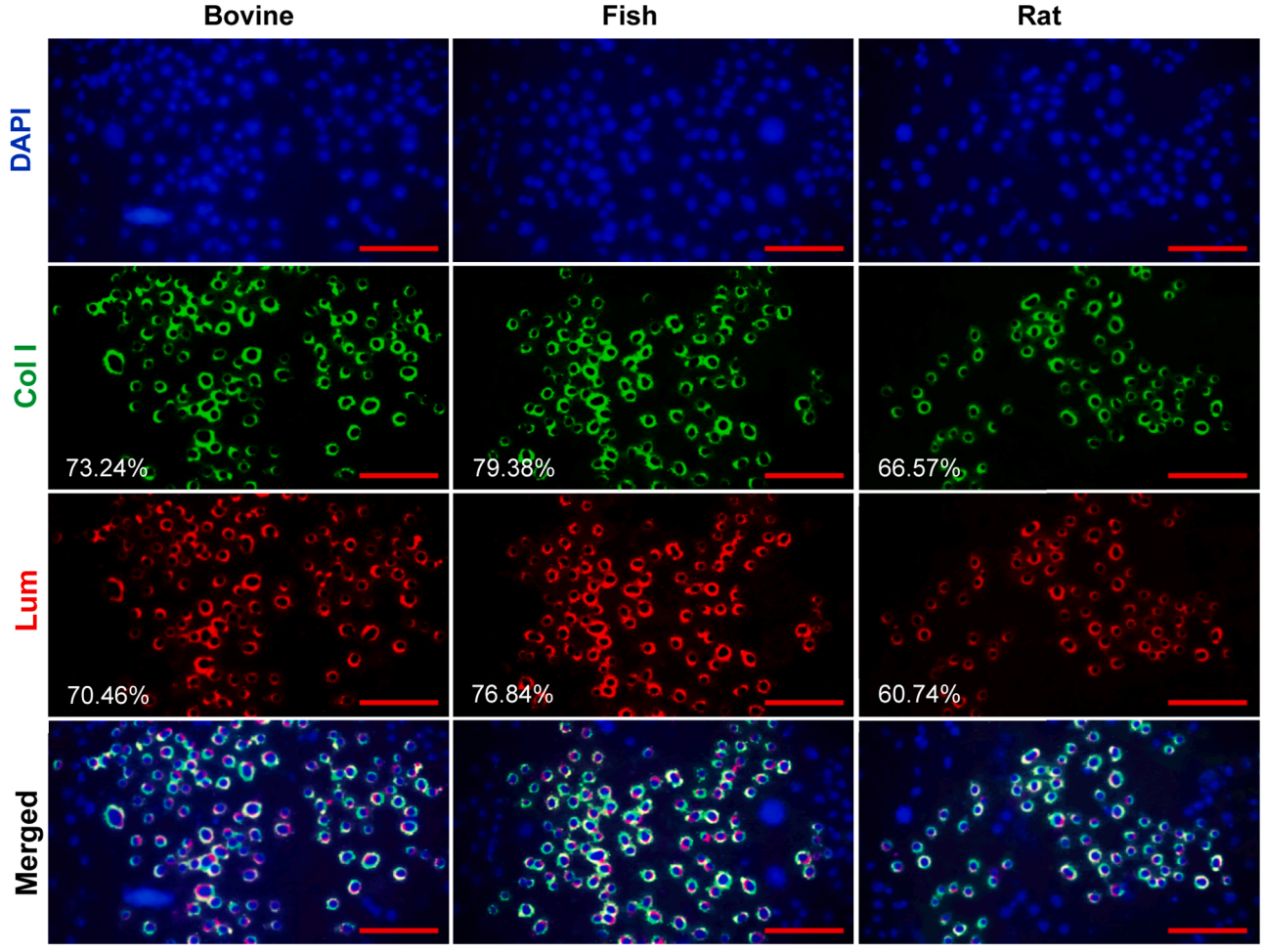

Fig. 6. Gene expression of seeded cells on optimized bicomponent hydrogels. Visualization and quantification of Col I and Lum protein secretion by hCSCs seeded on optimized ColMA/PEGDA hydrogels after 30 days (scale bar: 100 μm).

and rat tail tendons. It also highlighted the differences that the extraction source makes while using isolated collagens to fabricate photocrosslinked bicomponent hydrogels.

Here, isolation of type I collagen was carried out based on the solubility of collagen in dilute acidic solutions. The fish skin and rat tail tendons were completely dissolved in dilute acetic acid, but, in the case of bovine tendon, pepsin had to be added to the acidic solution to increase solubility, and, consequently, the yield of extraction process. Use of pepsin leads to the removal of telopeptide regions via cleavage of ketoimine crosslinks and increases collagen solubility [23]. The macroscopic appearance of the bulk collagens isolate from each source was similar in the dried state. Their major constituents that appeared in SDS-PAGE patterns were also similar and consisted of two α-chains (α_1 and α_2) (Fig. 1A). In this assay, after destroying protein structure, its reactive components were separated according to their molecular weight based on their different electrophoretic mobility. A decrease in β and γ bands was observed for bovine collagen, which was the evidence of cleavage of crosslinks by pepsin. UV/VIS absorption and FTIR spectra verified the purity of extracted collagens. The UV/VIS spectra for all samples exhibited a maximum absorption peak at 233 nm and a small one at 280 nm (Fig. 1B). The small peak at 280 nm is due to the presence of aromatic amino acids, *i.e.* tryptophan, tyrosine, and phenylalanine, in the extracted collagens [47]. Whereas, previous studies have shown that the triple helical structure of collagen has the maximum absorbance peak at 230-240 nm, which might be related to the accessibility of the groups C=O,–COOH, and $CONH_2$ in polypeptides chains of collagen [47–49]. FTIR spectra obtained for each collagen also presented typical bands of type I collagen, i.e. amide A, amide B, amide I, amide II, and amide III (Fig. 1C). The amide A band represented the hydrogen bond formation between the N-H group and a carbonyl group of the peptide chain [35]. The amide B band indicated the asymmetrical stretching of CH_2 [35]. The secondary structures of the extracted collagens were confirmed by observing amide I around 1653 cm^{-1}, which indicated the C=O stretching vibration along the polypeptide backbone [50]. Amide II and amide III were also associated with N–H bending vibrations coupled with C–N stretching vibration and C–H stretching, respectively [51]. Moreover, an absorption ratio greater than 0.95 was obtained between the amide III band and 1452 cm^{-1} band in the FTIR spectra of each collagen which confirmed the preservation of triple helices of the extracted collagens [52]. Triple helical structure is an important molecular feature of collagen, which affects its stability, strength, and biofunctionality [53]. Hence, the preservation of triple helical organization of extracted collagen was also addressed via CD spectroscopy (Fig. 1D). The spectra obtained for each sample represented a positive band around 221 nm and a large negative peak around 198 nm, which are associated with triple helices and polyproline chains of collagen, respectively [53]. For denatured collagen, these peaks diminished [54].

In the next step, the extracted collagens were functionalized with methacrylic anhydride to prepare photoreactive biomaterials. In this way, collagen lysine residues were covalently functionalized with methacrylic moieties without altering its triple helical conformation. ^1H NMR confirmed the covalent functionalization of collagen regardless of its sources. Obtained spectra (Fig. 2A) displayed the characteristic acrylic proton peaks of methacryl groups (5-6.5 ppm [19,29]). However, the DOM was different between sources that may be due to the different solubility of isolated collagens. Previous investigations revealed that collagen extraction source, as well as extraction method (with or without using pepsin), influenced the solubility of collagen at various pH [12]. After methacrylation, to improve the mechanical strength, ColMA from each source was used in combination with PEGDA to form a photocrosslinked bicomponent network, and the properties of *in situ* forming hydrogels were compared. The engineered hydrogels were synthesized through mixing photoreactive biopolymers (ColMA/PEGDA) with biocompatible photoinitiators (EY/TEA/NVP) that were activated with visible light using a dental light curing unit (wavelength of 440-490 nm). Methacrylated collagen derived from different sources was used in fabricating bicomponent hydrogels to compare the effect of collagen sources on the physicochemical properties of hydrogels and the behaviour of cells seeded on them *in vitro*.

It has been reported that in a visible light crosslinking system based on free radical chain reaction polymerization, the fully crosslinked hydrogel network cannot be obtained [55]. In this way, the physical, morphological, and mechanical properties of the engineered hydrogel and, consequently, its cellular behaviour can be altered by changing crosslinking parameters. Morphological features of scaffolds, including pore size and porosity, play a key role in modulating the properties of engineered tissues. Cellular penetration and the extent of ECM secretion increase by increasing the pore size and porosity. While enhancement of matrix porosity decreases matrix stiffness [56]. Here, at a fixed concentration of photoinitiator, three different light exposure times (30, 60, and 90 seconds) were considered, and its effect on the morphological features, mechanical strength, and cytocompatibility of bicomponent hydrogels containing ColMA from different sources was evaluated.

The presented results indicated that at a constant photoinitiator concentration, increasing light exposure time decreased the apparent pore size and porosity of hydrogels (Fig. 3D&E), which might be due to the enhancement of the degree of photocrosslinking. It is worth mentioning that lyophilization of the hydrogels prior to SEM analysis could increase the apparent porosity and pore size of the hydrogels. The mechanical strength of photocrosslinked ColMA/PEGDA hydrogels was also tuned by changing light exposure time. Results showed that bicomponent hydrogels exhibited tuneable Young's moduli in the range of 17-46 kPa (Fig. 3B), depending on collagen extraction source and light exposure time. Enhancement of the degree of crosslinking as a result of increasing light exposure time improved hydrogel stiffness. These observations are in agreement with previous studies based on engineering dental light curable GelMA hydrogels [57]. The effect of varying light exposure time on the cytocompatibility of engineered bicomponent hydrogels was also investigated (Fig. 3C). Supporting cell viability is one of the basic requirements of a scaffold for tissue engineering. Therefore, the suitability of the engineered photocrosslinked bicomponent hydrogels as a matrix to support *in vitro* viability of hCSCs was evaluated. The MTT assay was used to calculate cell viability by determining the percentage of viable cells seeded on the hydrogel surface with respect to those seeded on the culture plate. The results demonstrated that all kinds of hydrogel not only maintained the viability of hCSCs but also supported cell proliferation for up to 7 days as confirmed by cell viability of more than 120%. However, light exposure time had no statistically significant effect on cell viability. Hence, based on such observations and results obtained from mechanical stiffness and morphological features, the photocrosslinked hydrogels fabricated under visible light exposure for 60 seconds were used for all comparative experiments between collagen extraction sources.

Enzymatic degradation is an important factor for the determination of hydrogel stability once implanted *in vivo*. Evaluating the effect of collagen extraction source on hydrogel degradation indicated that hydrogels containing fish skin collagen degraded more quickly after incubation in collagenase type I solution (Fig. 4B). This was in good agreement with previous research that reported hydrogels based on marine collagen showed the least stability in enzyme solutions [10]. The compressive modulus of the bicomponent hydrogels also revealed that fish-based ColMA/PEGDA hydrogels had the lowest mechanical stiffness (Fig. 4A). One possible reason for such a difference can be due to the lower DOM of fish collagen as the DOM directly affects the compressive modulus of photocrosslinked hydrogels [58,59]. In addition, as reported by Carvalho et al. [40] fish collagen contains a lower number of imino acids, i.e. proline and hydroxyproline, compared to the other two collagens. It has been reported that the presence of proline and hydroxyproline residues in collagen structure increases its stiffness and elasticity, respectively [60]. The lower DOM of collagen extracted from fish skin also affected the effective swelling ratio of the photocrosslinked hydrogel. In comparison to hydrogels based on rat and bovine collagens,

hydrogels based on fish skin collagen showed a significantly higher swelling ratio (Fig. 4C). Bovine ColMA also had a lower DOM than rat ColMA; however, in comparison to rat-based hydrogels, the pore size of bovine-based hydrogels was smaller which may limit the water uptake of the hydrogels. A similar observation has been reported for genipin-crosslinked gelatine scaffolds wherein a reduction in pore size led to a noticeable decrease in swelling ratio [61].

Supporting 2D and 3D cell attachment and viability is an important property for hydrogels used in tissue engineering. After synthesis of the bicomponent ColMA/PEGDA hydrogels, collagen still contains the majority of its cell adhesion motif, i.e. RGD, to support cell attachment. Hence, hCSCs were seeded on the surface of hydrogels, and the attachment, viability, and proliferation of seeded cells were examined via MTT and live/dead assays at specific time points. The presented results from the MTT assay indicated that all hydrogels regardless of the collagen extraction source supported cell viability and proliferation (Fig. 5A). However, cells proliferated better on bovine-based hydrogels, which may be due to the bovine collagen amino acid composition. Park et al. [11] reported that the amino acid components of extracted collagen could affect *in vitro* cell behaviour. Live/dead assay also indicated that most of the seeded cells were alive and spread on the surface of bicomponent hydrogels. On the other hand, it was observed that rat- and fish-based hydrogels supported cell spreading better. Similar results were obtained for the spreading of hDPSCs seeded on the surface of bicomponent hydrogels (Fig. S3, Supplementary Material). Also, evaluating the cell migration within bicomponent hydrogels after 24 hours of incubation indicated that cells penetrated significantly better within fish- and rat-based hydrogels (Fig. 5B) possibly due to the larger pore size and porosity of these two compared to bovine-based hydrogels (Fig. 5C). Cell migration is undeniably essential for successful tissue repair/regeneration. Quantification was done by measuring the number of cells migrated as well as the distance they traveled into the hydrogels [62].

To evaluate the effect of collagen extraction source on the gene expression of hCSCs, the expression of Col I and Lum was examined via immunohistochemistry after 30 days of *in vitro* culturing (Fig. 6). Type I collagen is a major component of corneal stroma that controls its morphologies [63]. While Lum is a proteoglycan that regulates the arrangement and assembly of collagen matrix and plays a key role in the wound healing process in corneal stromal tissue [64]. In addition to the difference in amino acid composition, Zhang et al. [65] reported that scaffold properties such as surface topography and mechanical cues can influence the expression level of Col I and Lum in primary CSCs. Similarly, in this study, it was observed that differences in scaffold properties that came from collagen extraction sources affected Lum and Col I expression levels. The greatest and the lowest expression level of both Col I and Lum were observed in fish- and rat-based hydrogel groups, respectively. A comparative study between collagens extracted from the skin of chum salmon and porcine collagen also led to similar results where human periodontal ligament fibroblasts showed more differentiation activities on marine collagen hydrogels [66]. The presented observations obtained from cellular studies showed that ColMA/PEGDA hydrogels regardless of collagen extraction source had great biocompatibility and supported cell attachment, viability, proliferation, and gene expression. Fish skin-based hydrogels provided a slightly better environment for hCSCs to proliferate and express their related genes. Further investigations, especially *in vivo* tests, are required to evaluate the long-term performance of such constructs in clinical settings.

5. Conclusion

Type I collagen was extracted from three different animal sources, namely bovine Achilles tendon, bighead carp fish skin, and rat tail tendons, and the properties of photocrosslinked ColMA/PEGDA hydrogels based on different sources were comparatively investigated for use as the scaffold in tissue engineering applications. When using collagen as the basis of scaffolds, stability at physiological conditions, mechanical strength, and low risk of disease transmission are key elements that should be considered. The presented results indicated that data reported for a collagen-based scaffold may not directly be transferable to one based on collagen from a different species, mainly due to the different properties. Here, bicomponent hydrogels based on collagen extracted from fish skin showed less stability and mechanical strength, while Col I and Lum gene expression of hCSCs was the greatest when seeded on this type of hydrogel. In contrast, cells penetrated more easily within the hydrogel based on rat collagen, demonstrating the superiority of rat collagen over the other two collagens for use in cell homing-based tissue engineering approaches. The current study did not compare the biological performance of bicomponent hydrogels *in vivo*. Further studies are required to investigate the effect of collagen extraction sources on biological responses in clinical settings and to determine the suitability of fabricated bicomponent hydrogels for use in regenerative medicine.

Declaration of Competing Interest

The authors declare that they have no known competing financial interests or personal relationships that could have appeared to influence the work reported in this paper.

Acknowledgments

This work was supported by the National Institute for Medical Research Development (NIMAD) (grant numbers 972809, 983296). The authors wish to thank Drs. E. Shirzaei Sani and H. Capella-Monsonís for their valuable comments and suggestions.

Supplementary materials

Supplementary material associated with this article can be found, in the online version, at doi:10.1016/j.mtla.2022.101651.

References

[1] K.Y. Lee, D.J. Mooney, Hydrogels for tissue engineering, Chem. Rev. 101 (2001) 1869–1879.
[2] F.J. O'Brien, Biomaterials & scaffolds for tissue engineering, Mater. Today. 14 (2011) 88–95.
[3] P.X. Ma, Biomimetic materials for tissue engineering, Adv. Drug Deliv. Rev. 60 (2008) 184–198.
[4] J.H. Shim, J.Y. Kim, M. Park, J. Park, D.W. Cho, Development of a hybrid scaffold with synthetic biomaterials and hydrogel using solid freeform fabrication technology, Biofabrication 3 (2011), 034102.
[5] J. Lannutti, D. Reneker, T. Ma, D. Tomasko, D. Farson, Electrospinning for tissue engineering scaffolds, Mater. Sci. Eng. C. 27 (2007) 504–509.
[6] M.W. Tibbitt, K.S. Anseth, Hydrogels as extracellular matrix mimics for 3D cell culture, Biotechnol. Bioeng. 103 (2009) 655–663.
[7] E. Shirzaei Sani, R. Portillo Lara, Z. Aldawood, S.H. Bassir, D. Nguyen, A. Kantarci, G. Intini, N. Annabi, An antimicrobial dental light curable bioadhesive hydrogel for treatment of peri-implant diseases, Matter 1 (2019) 926–944.
[8] S. Mantha, S. Pillai, P. Khayambashi, A. Upadhyay, Y. Zhang, O. Tao, H.M. Pham, S.D. Tran, Smart hydrogels in tissue engineering and regenerative medicine, Materials (Basel) 12 (2019) 33.
[9] B. Chang, N. Ahuja, C. Ma, X. Liu, Injectable scaffolds: preparation and application in dental and craniofacial regeneration, Mater. Sci. Eng. R Reports. 111 (2017) 1–26.
[10] Y.K. Lin, D.C. Liu, Comparison of physical-chemical properties of type I collagen from different species, Food Chem. 99 (2006) 244–251.
[11] S.H. Park, T. Song, T.S. Bae, G. Khang, B.H. Choi, S.R. Park, B.H. Min, Comparative analysis of collagens extracted from different animal sources for application of cartilage tissue engineering, Int. J. Precis. Eng. Manuf. 13 (2012) 2059–2066.
[12] W. Jankangram, S. Chooluck, B. Pomthong, Comparison of the properties of collagen extracted from dried jellyfish and dried squid, African J. Biotechnol. 15 (2016) 642–648.
[13] C.M. Smith, A.L. Stone, R.L. Parkhill, R.L. Stewart, M.W. Simpkins, A.M. Kachurin, W.L. Warren, S.K. Williams, Three-dimensional bioassembly tool for generating viable tissue-engineered constructs, Tissue Eng. 10 (2004) 1566–1576.
[14] A.D. Nocera, N.A. Salvatierra, M.P. Cid, Printing collagen 3D structures, IFMBE Proc 49 (2015) 136–139.
[15] C. Mandrycky, Z. Wang, K. Kim, D.H. Kim, 3D bioprinting for engineering complex tissues, Biotechnol. Adv. 34 (2016) 422–434.

[16] S.V. Murphy, A. Skardal, A. Atala, Evaluation of hydrogels for bio-printing applications, J. Biomed. Mater. Res. - Part A. 101 A (2013) 272–284.
[17] M.G. Yeo, G.H. Kim, A cell-printing approach for obtaining hASC-laden scaffolds by using a collagen/polyphenol bioink, Biofabrication 9 (2017), 025004.
[18] Y.S. Kwon, S.H. Lee, Y.C. Hwang, V. Rosa, K.W. Lee, K.S. Min, Behaviour of human dental pulp cells cultured in a collagen hydrogel scaffold cross-linked with cinnamaldehyde, Int. Endod. J. 50 (2017) 58–66.
[19] I.D. Gaudet, D.I. Shreiber, Characterization of methacrylated type-I collagen as a dynamic, photoactive hydrogel, Biointerphases 7 (2012) 25.
[20] W.T. Brinkman, K. Nagapudi, B.S. Thomas, E.L. Chaikof, Photo-cross-linking of type I collagen gels in the presence of smooth muscle cells: mechanical properties, cell viability, and function, Biomacromolecules 4 (2003) 890–895.
[21] A. Mazzocchi, M. Devarasetty, R. Huntwork, S. Soker, A. Skardal, Optimization of collagen type I-hyaluronan hybrid bioink for 3D bioprinted liver microenvironments, Biofabrication 11 (2021), 015003.
[22] C.C. Clark, J. Aleman, L. Mutkus, A. Skardal, A mechanically robust thixotropic collagen and hyaluronic acid bioink supplemented with gelatin nanoparticles, Bioprinting 16 (2019) e00058.
[23] L.M. Delgado, N. Shologu, K. Fuller, D.I. Zeugolis, Acetic acid and pepsin result in high yield, high purity and low macrophage response collagen for biomedical applications, Biomed. Mater. 12 (2017), 065009.
[24] J. Li, M. Wang, Y. Qiao, Y. Tian, J. Liu, S. Qin, W. Wu, Extraction and characterization of type I collagen from skin of tilapia (Oreochromis niloticus) and its potential application in biomedical scaffold material for tissue engineering, Process Biochem. 74 (2018) 156–163.
[25] N. Rajan, J. Habermehl, M.F. Coté, C.J. Doillon, D. Mantovani, Preparation of ready-to-use, storable and reconstituted type I collagen from rat tail tendon for tissue engineering applications, Nat. Protoc. 1 (2007) 2753–2758.
[26] H. Capella-Monsonís, J.Q. Coentro, V. Graceffa, Z. Wu, D.I. Zeugolis, An experimental toolbox for characterization of mammalian collagen type I in biological specimens, Nat. Protoc. 13 (2018) 507–529.
[27] C.B. Raub, V. Suresh, T. Krasieva, J. Lyubovitsky, J.D. Mih, A.J. Putnam, B. J. Tromberg, S.C. George, Noninvasive assessment of collagen gel microstructure and mechanics using multiphoton microscopy, Biophys. J. 92 (2007) 2212–2222.
[28] V, MG, JB, Specification Sheet- ColMA Solution, 2020. www.cellink.com.
[29] C. Claaßen, M.H. Claaßen, V. Truffault, L. Sewald, G.E.M. Tovar, K. Borchers, A. Southan, Quantification of substitution of gelatin methacryloyl: best practice and current pitfalls, Biomacromolecules 19 (2018) 42–52.
[30] W. Schuurman, P.A. Levett, M.W. Pot, P.R. van Weeren, W.J.A. Dhert, D. W. Hutmacher, F.P.W. Melchels, T.J. Klein, J. Malda, Gelatin-methacrylamide hydrogels as potential biomaterials for fabrication of tissue-engineered cartilage constructs, Macromol. Biosci. 13 (2013) 551–561.
[31] G. Unal, J. Jones, S. Baghdasarian, N. Kaneko, E. Shirzaei Sani, S. Lee, S. Gholizadeh, S. Tateshima, N. Annabi, Engineering elastic sealants based on gelatin and elastin-like polypeptides for endovascular anastomosis, Bioeng. Transl. Med. 6 (2021) e10240.
[32] Y. Zhang, Y.-C. Wang, O. Yuka, L. Zhang, C.-Y. Liu, Mouse corneal stroma fibroblast primary cell culture, Bio-Protocol 6 (2016) 1–5.
[33] S.S. Mahdavi, M.J. Abdekhodaie, H. Kumar, S. Mashayekhan, A. Baradaran-Rafii, K. Kim, Stereolithography 3D bioprinting method for fabrication of human corneal stroma equivalent, Ann. Biomed. Eng. 48 (2020) 1955–1970.
[34] W.-K. Song, D. Liu, L.-L. Sun, B.-F. Li, H. Hou, Physicochemical and biocompatibility properties of type I collagen from the skin of Nile tilapia (Oreochromis niloticus) for biomedical applications, Mar. Drugs. 17 (2019) 137.
[35] T. Riaz, R. Zeeshan, F. Zarif, K. Ilyas, N. Muhammad, S.Z. Safi, A. Rahim, S.A. A. Rizvi, I.U. Rehman, FTIR analysis of natural and synthetic collagen, Appl. Spectrosc. Rev. 53 (2018) 703–746.
[36] A. Veeruraj, M. Arumugam, T. Balasubramanian, Isolation and characterization of thermostable collagen from the marine eel-fish (Evenchelys macrura), Process Biochem. 48 (2013) 1592–1602.
[37] M.H. Santos, R.M. Silva, V.C. Dumont, J.S. Neves, H.S. Mansur, L.G.D. Heneine, Extraction and characterization of highly purified collagen from bovine pericardium for potential bioengineering applications, Mater. Sci. Eng. C. 33 (2013) 790–800.
[38] K. Belbachir, R. Noreen, G. Gouspillou, C. Petibois, Collagen types analysis and differentiation by FTIR spectroscopy, Anal. Bioanal. Chem. 395 (2009) 829–837.
[39] H. Jafari, A. Lista, M.M. Siekapen, P. Ghaffari-Bohlouli, L. Nie, H. Alimoradi, A. Shavandi, Fish collagen: Extraction, characterization, and applications for biomaterials engineering, Polymers (Basel) 12 (2020) 1–37.
[40] A.M. Carvalho, A.P. Marques, T.H. Silva, R.L. Reis, Evaluation of the potential of collagen from codfish skin as a biomaterial for biomedical applications, Mar. Drugs. 16 (2018).
[41] J.H. Bowes, R.G. Elliott, J.A. Moss, The composition of collagen and acid-soluble collagen of bovine skin, Biochem. J. 61 (1955) 143–150.
[42] X.L. Chen, M. Peng, J. Li, B.L. Tang, X. Shao, F. Zhao, C. Liu, X.Y. Zhang, P.Y. Li, M. Shi, Y.Z. Zhang, X.Y. Song, Preparation and functional evaluation of collagen oligopeptide-rich hydrolysate from fish skin with the serine collagenolytic protease from Pseudoalteromonas sp. SM9913, Sci. Rep. 7 (2017) 1–13.
[43] G. Tronci, S.J. Russell, D.J. Wood, Photo-active collagen systems with controlled triple helix architecture, J. Mater. Chem. B. 1 (2013) 3705–3715.
[44] Y. Feng, G. Melacini, J.P. Taulane, M. Goodman, Acetyl-terminated and template-assembled collagen-based polypeptides composed of Gly-Pro-Hyp sequences. 2. Synthesis and conformational analysis by circular dichroism, ultraviolet absorbance, and optical rotation, J. Am. Chem. Soc. 118 (1996) 10351–10358.
[45] F. Felician, C. Xia, W. Qi, H. Xu, Collagen from marine biological sources and medical applications, Chem. Biodivers. 15 (2018).
[46] A.K. Lynn, I.V. Yannas, W. Bonfield, Antigenicity and immunogenicity of collagen, J. Biomed. Mater. Res. - Part B Appl. Biomater. 71 (2004) 343–354.
[47] G.K. Pal, P.V. Suresh, Physico-chemical characteristics and fibril-forming capacity of carp swim bladder collagens and exploration of their potential bioactive peptides by in silico approaches, Int. J. Biol. Macromol. 101 (2017) 304–313.
[48] W.H. Zhao, C.F. Chi, Y.Q. Zhao, B. Wang, Preparation, physicochemical and antioxidant properties of acid- and pepsin-soluble collagens from the swim bladders of miiuy croaker (Miichthys miiuy), Mar. Drugs. (2018) 16.
[49] D. Yu, C.F. Chi, B. Wang, G.F. Ding, Z.R. Li, Characterization of acid-and pepsin-soluble collagens from spines and skulls of skipjack tuna (Katsuwonus pelamis), Chin, J. Nat. Med. 12 (2014) 712–720.
[50] C.F. Chi, B. Wang, Z.R. Li, H.Y. Luo, G.F. Ding, C.W. Wu, Characterization of acid-soluble collagen from the skin of hammerhead shark (Sphyrna lewini), J. Food Biochem. 38 (2014) 236–247.
[51] S. Tamilmozhi, A. Veeruraj, M. Arumugam, Isolation and characterization of acid and pepsin-solubilized collagen from the skin of sailfish (Istiophorus platypterus), Food Res. Int. 54 (2013) 1499–1505.
[52] Z.R. Li, B. Wang, C. feng Chi, Q.H. Zhang, Y. dan Gong, J.J. Tang, H. yu Luo, G. fang Ding, Isolation and characterization of acid soluble collagens and pepsin soluble collagens from the skin and bone of Spanish mackerel (Scomberomorous niphonius), Food Hydrocoll. 31 (2013) 103–113.
[53] G. Tronci, C.A. Grant, N.H. Thomson, S.J. Russell, D.J. Wood, Multi-scale mechanical characterization of highly swollen photo-activated collagen hydrogels, J. R. Soc. Interface. 12 (2015).
[54] H. Mori, Y. Tone, K. Shimizu, K. Zikihara, S. Tokutomi, T. Ida, H. Ihara, M. Hara, Studies on fish scale collagen of Pacific saury (Cololabis saira), Mater. Sci. Eng. C. 33 (2013) 174–181.
[55] C.C. Lin, C.S. Ki, H. Shih, Thiol-norbornene photoclick hydrogels for tissue engineering applications, J. Appl. Polym. Sci. 132 (2015) 1–11.
[56] N. Annabi, J.W. Nichol, X. Zhong, C. Ji, S. Koshy, A. Khademhosseini, F. Dehghani, Controlling the porosity and microarchitecture of hydrogels for tissue engineering, Tissue Eng. Part B. 16 (2010) 371–383.
[57] N. Monteiro, G. Thrivikraman, A. Athirasala, A. Tahayeri, C.M. França, J. L. Ferracane, L.E. Bertassoni, Photopolymerization of cell-laden gelatin methacryloyl hydrogels using a dental curing light for regenerative dentistry, Dent. Mater. 34 (2018) 389–399.
[58] D.F. Coutinho, S. Sant, H. Shin, J.T. Oliveira, M.E. Gomes, N.M. Neves, A. Khademhosseini, R.L. Reis, Modified Gellan Gum hydrogels with tunable physical and mechanical properties, Biomaterials 31 (2010) 7494–7502.
[59] S.A. Bencherif, A. Srinivasan, F. Horkay, J.O. Hollinger, K. Matyjaszewski, N. R. Washburn, Influence of the degree of methacrylation on hyaluronic acid hydrogels properties, Biomaterials 29 (2008) 1739–1749.
[60] A. Ghanaeian, R. Soheilifard, Mechanical elasticity of proline-rich and hydroxyproline-rich collagen-like triple-helices studied using steered molecular dynamics, J. Mech. Behav. Biomed. Mater. 86 (2018) 105–112.
[61] S.M. Lien, L.Y. Ko, T.J. Huang, Effect of pore size on ECM secretion and cell growth in gelatin scaffold for articular cartilage tissue engineering, Acta Biomater. 5 (2009) 670–679.
[62] N. Kramer, A. Walzl, C. Unger, M. Rosner, G. Krupitza, M. Hengstschläger, H. Dolznig, In vitro cell migration and invasion assays, Mutat. Res. - Rev. Mutat. Res. 752 (2013) 10–24.
[63] K.M. Meek, N.J. Fullwood, Corneal and scleral collagens - A microscopist's perspective, Micron 32 (2001) 261–272.
[64] E.C. Carlson, C.Y. Liu, T.I. Chikama, Y. Hayashi, C.W.C. Kao, D.E. Birk, J. L. Funderburgh, J.V. Jester, W.W.Y. Kao, Keratocan, a cornea-specific keratan sulfate proteoglycan, is regulated by lumican, J. Biol. Chem. 280 (2005) 25541–25547.
[65] W. Zhang, J. Chen, L.J. Backman, A.D. Malm, P. Danielson, Surface topography and mechanical strain promote keratocyte phenotype and extracellular matrix formation in a biomimetic 3D corneal model, Adv. Healthc. Mater. 6 (2017).
[66] N. Nagai, K. Mori, Y. Satoh, N. Takahashi, S. Yunoki, K. Tajima, M. Munekata, In vitro growth and differentiated activities of human periodontal ligament fibroblasts cultured on salmon collagen gel, Biomaterials 82 (2007) 395–402.